RESEARCH ARTICLE   https://doi.org/10.1158/2767-9764.CRC-24-0442   OPEN ACCESS

APOBEC3 Activity Promotes the Survival and Evolution of Drug-Tolerant Persister Cells during EGFR Inhibitor Resistance in Lung Cancer

Nina Marie G. Garcia[1,2], Jessica N. Becerra[1], Sharan Srinivasan[1], Brock J. McKinney[1], Ashley V. DiMarco[2], Feinan Wu[3], Matthew Fitzgibbon[3], and James V. Alvarez[1]

ABSTRACT

APOBEC mutagenesis is one of the most common endogenous sources of mutations in human cancer and is a major source of genetic intra-tumor heterogeneity. High levels of APOBEC mutagenesis are associated with poor prognosis and aggressive disease across diverse cancers, but the mechanistic and functional impacts of APOBEC mutagenesis on tumor evolution and therapy resistance remain relatively unexplored. To address this, we investigated the contribution of APOBEC mutagenesis to acquired therapy resistance in a model of EGFR-mutant non–small cell lung cancer. We find that inhibition of EGFR in lung cancer cells leads to a rapid and pronounced induction of APOBEC3 expression and activity. Functionally, APOBEC expression promotes the survival of drug-tolerant persister cells (DTP) following EGFR inhibition. Constitutive expression of APOBEC3B alters the evolutionary trajectory of acquired resistance to the EGFR inhibitor gefitinib, making it more likely that resistance arises through *de novo* acquisition of the T790M gate-keeper mutation and squamous transdifferentiation during the DTP state. APOBEC3B expression is associated with increased expression of

the squamous cell transcription factor ΔNp63 and squamous cell trans-differentiation in gefitinib-resistant cells. Knockout of p63 in gefitinib-resistant cells reduces the expression of the ΔNp63 target genes IL-1α/β and sensitizes these cells to the third-generation EGFR inhibitor osimertinib. These results suggest that APOBEC activity promotes acquired resistance by facilitating evolution and transdifferentiation in DTPs and that approaches to target ΔNp63 in gefitinib-resistant lung cancers may have therapeutic benefit.

Significance: APOBEC mutagenesis is a common source of genetic heterogeneity in cancer, and APOBEC mutational signatures are enriched in metastatic and drug-resistant tumors. However, the mechanisms through which APOBEC3 enzymes promote tumor evolution remain unknown. In this study, we show that APOBEC3 activity contributes to the development of therapy-resistant cancer cells by promoting evolution of DTP cells. These findings offer insights into the role of APOBEC mutagenesis in cancer progression.

Introduction

The APOBEC mutational signature, characterized by C-to-T transitions and C-to-G transversions occurring in a TpCpW context, is a prominent mutational process in multiple tumor types, including lung adenocarcinomas (1–5). APOBEC mutagenesis results from the activity of the APOBEC3A and APOBEC3B enzymes, which deaminate cytosines on single-stranded DNA (6–9). APOBEC mutagenesis and expression of *APOBEC3A* and *APOBEC3B* genes are associated with poor prognosis and intratumor heterogeneity and are

increased in metastatic and drug-resistant tumors (10–14). Therefore, eluci-dating the functional consequences of APOBEC mutagenesis on tumor pro-gression, and the mechanisms underlying these effects, is an important goal.

To address these issues, we examined the role of APOBEC mutagenesis in acquired resistance to EGFR inhibitors in EGFR-mutant lung cancer. First-generation EGFR inhibitors, such as gefitinib and erlotinib, exhibit activity in patients with non–small cell lung cancers (NSCLC) harboring activating mutations in EGFR (15–17). However, nearly all patients will develop re-sistance to these targeted therapies, limiting treatment options for these patients (18–20). Consequently, it is important to identify and characterize mechanisms of acquired drug resistance to EGFR inhibitors. The most common mechanisms of resistance are secondary mutations in the *EGFR* gene itself, including the T790M mutation, which prevents drug binding and allows persistent EGFR activity even in the presence of drug (21, 22). In this subset of patients, third-generation EGFR inhibitors, such as osimertinib, are often the next treatment option (23). A number of other genetic resistance mechanisms have been discovered, including amplification or mutation of other receptor tyrosine kinases, including *MET*, fibroblast growth factor receptor, *HER2*, and anaplastic lymphoma kinase (24–27). Several

[1]Translational Research Program, Public Health Sciences Division, Fred Hutchinson Cancer Center, Seattle, Washington. [2]Department of Pharmacology and Cancer Biology, Duke University School of Medicine, Durham, North Carolina. [3]Genomics and Bioinformatics, Fred Hutchinson Cancer Center, Seattle, Washington.

Corresponding Author: James V. Alvarez, Fred Hutchinson Cancer Center, 1100 Fairview Avenue N, M5-C803, Seattle, WA 98109. E-mail: jalvarez@fredhutch.org

nongenetic resistance mechanisms have also been described, including the epithelial-to-mesenchymal transition (refs. 28–30) and histologic transformation to other lung cancer cell types, such as small cell lung cancer (SCLC) and squamous cell carcinoma (SCC; refs. 31–33). The cellular and molecular pathways underlying histologic transformation remain unknown, and importantly, there are currently no therapies available for patients who develop resistance to EGFR inhibitors via transdifferentiation to a small cell or squamous cell phenotype.

Interestingly, the APOBEC mutational signature is elevated in tumors from patients who have undergone treatment with EGFR inhibitors and developed acquired resistance to these inhibitors (34). Among these patients, APOBEC signatures are especially high in tumors that have acquired resistance through histologic transformation (35, 36). Recent work has found that *APOBEC3A* and *APOBEC3B* genes are induced by anti-EGFR targeted therapy and contribute to the acquisition of drug resistance (37, 38). However, the precise mechanism by which APOBEC3 enzymes promote resistance to EGFR inhibitors remains unclear. In addition, the relationship between APOBEC mutagenesis and transdifferentiation remains unexplored. In the current study, we explore the regulation and function of APOBEC mutagenesis during acquired resistance to EGFR inhibitors. We find that EGFR inhibition induces APOBEC3 expression and activity, which in turn promotes the survival of drug-tolerant persister cells (DTP). Sustained APOBEC3B expression promotes the evolution of drug resistance in DTPs and is associated with squamous cell transdifferentiation in EGFR inhibitor–resistant cells. These findings reveal an important role for APOBEC activity in the evolution of drug resistance.

Materials and Methods

Tissue culture and reagents

Cell lines

PC9, HCC827, and BT474 cells were grown in RPMI-1640 media containing 10% FBS, L-glutamine, and penicillin/streptomycin. SKBR3 cells were grown in DMEM containing 10% FBS, L-glutamine, and penicillin/streptomycin. Lentivirus from HEK293T cells was produced as previously described (39). Cells were selected using puromycin or blasticidin, as indicated.

Generation of Cre-inducible A3B expression in PC9 cells

To create a Cre-inducible A3B construct, we used an approach based upon the XTR system (40). Briefly, the human A3B coding sequence (NM_004900.4) with a C-terminal HA tag and an SV40 intron was cloned downstream of the human PGK promoter in the reverse orientation. This reverse A3B-HA cDNA was flanked by two pairs of incompatible loxP sites (Lox5171 and Lox2722), such that expression of Cre recombinase leads to inversion of the A3B cDNA and expression of the full-length A3B gene. This construct, pLenti-APOBEC3B-Intron-HA-Cre Flp, was generated by VectorBuilder. Polyclonal populations of cells with Cre-induced A3B expression were used for all experiments.

CRISPR/Cas9-mediated knockout

lentiCas9-Blast was a gift from Feng Zhang (Addgene, plasmid #52962). For A3A and A3B knockout (KO), PC9 Cas9 cells were transduced with lentiviral constructs expressing dual single-guide RNAs (sgRNA), either nontargeting (NT1/NT2), A3A/NT1, A3B/NT1, or A3A/A3B. NT1 guide RNA (gRNA):

GGCAGTCGTTCGGTTGATAT; NT2 gRNA: GCTTGAGCACATACG-CGAAT; A3A gRNA: GTGCTGGTCCATCTTGACCG; and A3B gRNA: ATGACCCTTTGGTCCTTCGA. Dual-sgRNA vectors were generated by Cellecta. KO cells were selected using puromycin and then transduced with H2B-GFP lentivirus. GFP-positive KO cells were sorted using flow cytometry and single-cell clones were generated.

For TP63 knockout, gRNAs targeting TP63 were cloned into lentiCRISPR v2 (a gift from Feng Zhang; Addgene, plasmid #52961). An empty LCV2-Cas9 construct was used as a control. TP63 sgRNA 1: CAATGATTAAAATTG-GACGG and TP63 sgRNA 3: GCTGAGCCGTGAATTCAACG.

A3B expression and drug treatments

For expression of A3B, 2×10^5 PC9 Cre/Flp A3B cells were seeded onto a six-well plate. Twenty-four hours later, adenovirus expressing Cre recombinase (Vector Biolabs) was added to the media at a multiplicity of infection of 1,000. For short-term treatments, gefitinib (SelleckChem) was used at a concentration of 500 nmol/L and osimertinib (SelleckChem) was used at a concentration of 1 μmol/L. For long-term cell viability assays, PC9 cells were treated with 100 nmol/L osimertinib.

Knockdown experiments

SMARTpool ON-TARGETplus siRNAs for RELA, RELB, c-REL, IRF3, and STAT1 were purchased from Horizon Discovery. The DharmaFECT transfection protocol was followed as described. Briefly, PC9 cells were plated with antibiotic-free complete media and incubated overnight. After 24 hours, siRNA SMARTpools were resuspended and diluted to the desired concentration. They were then mixed with the transfection reagent (DharmaFECT) in serum-free media and brought up to volume with complete media. The transfection medium was added to the cells. The cells were then incubated with the transfection media for 24 hours. PC9 cells were treated with gefitinib or osimertinib 48 hours after transfection. The cells were harvested for subsequent experiments 24 hours after drug treatment.

Resistance assays

A total of 2×10^5 PC9 Cre/Flp A3B cells were seeded onto six-well plates. After 24 hours, AdenoCre recombinase (Vector Biolabs) was added to the media at a multiplicity of infection of 1,000. The cells were cultured for 3 weeks prior to treatment with gefitinib. After 3 weeks, 1×10^6 PC9 cells, with or without A3B expression, were seeded onto 10-cm plates. Twenty-four hours later, media were changed to media containing 100 nmol/L gefitinib. Media were changed every 3 days after treatment and the cells were counted and passaged every 7 days after treatment until the cells acquired resistance. Then 1×10^6 cells (or the entire culture if less than 1×10^6 cells) were re-plated at each passage. Gefitinib-resistant (GR) cells were cultured continuously in gefitinib-containing media. Calculated cell number was determined using the following formula:

$$\text{calculated cell} \# = (\text{previous calculated cell} \#) \times 2^{\text{cell generation}}$$

$$\text{cell generation} = \frac{\log(\text{cells per plate}) - \log(\text{cells replated})}{\log 2}$$

qRT-PCR

RNA was isolated from cells using RNeasy columns (Qiagen). Using cDNA synthesis reagents (Promega), 1 μg of RNA was reversed transcribed. qPCR

was performed using the following 6-carboxyfluorescein-labeled TaqMan probes (Thermo Fisher Scientific): APOBEC3A (Hs00377444_m1), APOBEC3B (Hs00358981_m1), ACTB (Hs01060665_g1), 18S (Hs03003631_g1), IL-1A (Hs00174092_m1), IL-1B (Hs01555410_m1), dN-TP63 (Hs00978339_m1), total TP63 (Hs00978340_m1), RELA (Hs01042014_m1), RELB (Hs00232399), C-REL (Hs00968440_m1), IRF3 (Hs01547283_m1), and STAT1 (Hs01013996_m1). qPCR was performed using an AB Applied Biosystems ViiA 7 qPCR machine.

Western blotting

Western blotting was performed as described (39) using the following antibodies: APOBEC3A/B/G (gift from Maciejowski Lab; ref. 9), actin (Cell Signaling Technology), HA-tag (Cell Signaling Technology), and α-tubulin (Cell Signaling Technology), all at a 1:1,000 dilution. Secondary antibodies conjugated to Alexa Fluor 680 (Life Technologies) or IR-800 (LI-COR Biosciences) were detected with the Odyssey detection system (LI-COR Biosciences). For endogenous A3B detection, secondary antibodies conjugated to horseradish peroxidase were used and blots were developed using Forte or Crescendo reagent (Millipore) and exposed to film (VWR). Secondary antibodies were used at a 1:5,000 dilution.

Deaminase assay

Deaminase assays were performed as previously described (39). % deamination was calculated using the following formula:

$$\% \, deamination = \frac{product \, signal}{substrate \, signal + product \, signal} \times 100$$

Droplet digital PCR

Genomic DNA (gDNA) was isolated using the DNeasy Blood and Tissue Kit (Qiagen). Each reaction contained the following: 10 ng gDNA, $EGFR^{T790M}$ probe (assay ID: dHsaCP2000019, Bio-Rad), wild-type EGFR probe (assay ID: dHsaCP2000020, Bio-Rad), HaeIII restriction enzyme (New England Biolabs), and ddPCR Supermix (no dUTPs; Bio-Rad). Onto a DG8 cartridge (Bio-Rad), 20 μL of each reaction was loaded, along with 70 μL of droplet generation oil (Bio-Rad). Droplets were generated using the Bio-Rad QX200 Droplet Digital PCR System and then transferred to a 96-well plate for PCR. PCR conditions were as follows: 95°C for 10 minutes, 40 cycles of 94°C for 30 seconds, followed by 55°C for 1 minute, and 98°C for 1 minute. Droplets were analyzed on the Bio-Rad QX200 Droplet Reader for FAM (T790M) and HEX (WT) probes. Data were analyzed with the Quanta-Soft software (Bio-Rad) to obtain fractional abundance of mutated gDNA. % $EGFR^{T790M}$ was calculated using the following formula:

$$\% \, EGFR \, T790M = \frac{copies \, T790M}{copies \, WT + T790M} \times 100$$

Competition assay and flow cytometry

GFP-labeled A3A/A3B double-KO clones were mixed with NT1/NT2 control cells in a 1:1 ratio and then seeded onto six-well plates. After 24 hours, the cells were treated with either 100 nmol/L gefitinitib or 500 nmol/L osimertinib. Media containing drug or vehicle were changed every 3 to 4 days. On days 7 and 14 after drug treatment, the ratio of GFP-positive to GFP-negative cells was measured using flow cytometry on a BD FACSCanto II flow cytometer.

RNA sequencing

RNA was isolated from cells using RNeasy columns (Qiagen). RNA sequencing (RNA-seq) was performed by Novogene. Briefly, mRNA was purified from total RNA using poly-T oligo-attached magnetic beads. After fragmentation, the first-strand cDNA was synthesized using random hexamer primers, followed by the second-strand cDNA synthesis using dTTP for non-directional library. Libraries were subjected to end-repair, A-tailing, adapter ligation, size selection, amplification, and purification. Quantified libraries were pooled and sequenced on NovaSeq PE150.

STAR v2.7.9a with two-pass mapping was used to align paired-end reads to human genome assembly hg38 and GENCODE gene annotation v38 along with gene-level read quantification. The Bioconductor package edgeR 3.36.0 was used to detect differential gene expression between sample groups. Protein-coding and long noncoding RNA genes were included in the analysis. Genes with low expression were excluded using the edgeR function filterByExpr with min.count = 10 and min.total.count = 15. The filtered expression matrix was normalized by the trimmed mean of M-values method and subjected to significance testing using the quasi-likelihood pipeline implemented in edgeR. For group comparisons, biological replicates were used as blocking factor (i.e., unwanted covariate) in the statistical model when applicable. A gene was deemed differentially expressed if absolute $\log_2$ fold change was above one (i.e., fold change >2 in either direction) and Benjamini–Hochberg–adjusted P value was less than 0.01.

Whole-exome sequencing

gDNA was isolated using the DNeasy Blood and Tissue Kit (Qiagen). The Twist Bioscience Whole-Exome Sequencing (WES) Kit was used for capture and library preparation and paired-end Illumina next-generation sequencing was performed using NextSeq 2000 according to the manufacturer's recommendations. Read processing and germline variant calling followed the GATK best practice workflow (https://gatk.broadinstitute.org/hc/en-us/articles/360035535932-Germline-short-variant-discovery-SNPs-Indels-). Known single-nucleotide variants and INDELs were retrieved from GATK resource bundle (https://console.cloud.google.com/storage/browser/genomics-public-data/resources/broad/hg38/v0;tab=objects?prefix=&forceOnObjectsSortingFiltering=false). Briefly, Illumina adapters were first trimmed from paired-end reads using cutadapt (http://dx.doi.org/10.14806/ej.17.1.200) and trimmed reads were mapped to the reference genome hg38 using BWA 0.7.17 (https://doi.org/10.1093/bioinformatics/btp324). Bam files were further processed using GATK 4.2.5 to generate analysis-ready reads that have proper read group information, duplicated reads marked (MarkDuplicates), and recalibrated base quality score (BaseRcalibrator and ApplyBQSR). GATK HaplotypeCaller was run in GVCF mode for each sample, followed by joint calling of all samples using GenomicsDBImport and GenotypeGVCFs. Twist panel–targeted regions were padded with 50 bp on both sides for the above processing and variant calling. As there were less than 30 samples in the cohort, variants were subjected to hard filtering by following the GATK article (https://gatk.broadinstitute.org/hc/en-us/articles/360035531112--How-to-Filter-variants-either-with-VQSR-or-by-hard-filtering#1).

Xenograft studies

Animal care and animal experiments were performed with the approval, and in accordance with the guidelines, of the Fred Hutchinson Cancer Center

Institutional Animal Care and Use Committee under Protocol #PROTO202100023. Into the flanks of nude mice (6–8 weeks old), 1×10^5 cells diluted in PBS:Matrigel (1:1) were injected subcutaneously. Tumors developed in 6 to 8 weeks and tumor volume was measured once a week using calipers. Established tumors were harvested and fixed in 10% neutral buffered formalin for 24 hours, washed in PBS, and then stored in 70% ethanol.

IHC

Staining was performed by the Experimental Histopathology core resource at Fred Hutchinson Cancer Center. For cell lines, 5×10^6 cells were harvested, washed in PBS, and fixed in 200 µL 10% neutral buffered formalin for 24 hours. Tumors were harvested and fixed in 10% neutral buffered formalin for 24 hours, washed with PBS, and then stored in 70% ethanol until staining. Tumor sections and cells were stained with p40 antibody (Abcam) to detect ΔNp63.

Statistics

Statistical analysis was performed using GraphPad Prism. Statistical tests used and *P* values are reported with each figure.

Data availability

RNA-seq and WES data are available online using NCBI's Short Read Archive under project accession number PRJNA1235703. Other data generated in this study are available within the article, its supplementary data files, or upon request from the corresponding author.

Results

APOBEC3 expression and activity are induced following EGFR inhibition

To explore the functional consequences of APOBEC mutagenesis on acquired resistance to EGFR inhibitors, we used PC9 cells, a NSCLC cell line that has an activating mutation in EGFR (exon 19 deletion). We first assessed change in the expression and activity of APOBEC3 genes in response to EGFR inhibition. The treatment of PC9 cells with the tyrosine kinase inhibitors (TKI) gefitinib or osimertinib led to induction of both the *APOBEC3A* (A3A) and *APOBEC3B* (A3B) genes (Fig. 1A). In a second EGFR-mutant NSCLC cell line, HCC827, A3A and A3B genes were also induced following treatment with gefitinib and osimertinib (Supplementary Fig. S1A). A3B protein levels also increased following treatment with these inhibitors (Fig. 1B) although we were unable to detect A3A protein. To assess the impact of EGFR inhibition on the enzymatic activity of APOBEC3 proteins, we used a deaminase activity assay that measures the ability of a lysate to deaminate a cytosine within an APOBEC consensus sequence in a single-stranded DNA oligonucleotide (41). Gefitinib or osimertinib treatment led to a two- to three-fold increase in deaminase activity (Fig. 1C and D). Together, these results suggest that EGFR inhibition in NSCLC cells leads to the induction of APOBEC expression and activity, consistent with previous findings (37, 38).

To investigate the pathways responsible for APOBEC3 induction, we used siRNA to knock down candidate transcription factors known to play a role in APOBEC3 expression. We first focused on the NF-κB pathway as these proteins have been shown to regulate APOBEC3 expression in diverse contexts (42–44). We found that knockdown of RelA did not affect the induction of A3A or A3B (Supplementary Fig. S1B), whereas knockdown of RelB or c-Rel partially blunted the upregulation of A3A and A3B following gefitinib or osimertinib treatment (Supplementary Fig. S1C and S1D). However, knockdown of these proteins only partially blocked A3A and A3B induction, suggesting that other pathways may contribute to the transcriptional upregulation of APOBEC3 in response to EGFR inhibition.

Other pathways that can activate A3A and A3B include the type-I IFN pathway, which signals through STAT transcription factors, and IRF3, which is activated as part of the innate immune response to viral infection (45–47). We therefore tested whether knockdown of STAT1 or IRF3 prevented A3A and A3B induction following EGFR inhibition. We found that STAT1 knockdown almost completely blocked the upregulation of A3A and A3B following EGFR inhibition (Supplementary Fig. S1E). In contrast, IRF3 blocked the upregulation of A3B but not A3A (Supplementary Fig. S1F). Taken together, these data identify several pro-inflammatory transcription factors, notably STAT1, that are required for the transcriptional upregulation of A3A and A3B following EGFR inhibition.

APOBEC3 expression promotes the survival of DTP cells following EGFR inhibition

To assess the impact of A3A and A3B upregulation on the response of lung cancer cells to EGFR inhibition, we used CRISPR/Cas9 to knock out each gene in PC9 cells. The cells were infected with lentivirus expressing Cas9 along with sgRNAs targeting A3A, A3B, or both, and following selection, individual clones were expanded and screened. Western blot analysis confirmed that two A3B-KO clones (B6 and F11) had reduced levels of A3B expression, both at baseline and following EGFR inhibition (Supplementary Fig. S2A). Because we could not detect A3A protein, we assessed A3A knockout by sequencing gDNA surrounding the sgRNA recognition site. Two A3A-KO clones (B10 and D3) had mutations predicted to partially (clone D3) or fully (clone B10) disrupt A3A expression (Supplementary Table S1). Using similar approaches, we identified two A3A/A3B double-KO clones (G10 and E2) with knockout of both A3A and A3B (Fig. 1E; Supplementary Table S1).

We first examined the induction of cytosine deaminase activity in these clones following EGFR inhibition. Knockout of A3B alone, as well as knockout of A3A and A3B together, led to a reduction in basal deaminase activity and blunted the increase in deaminase activity resulting from EGFR inhibition (Fig. 1F and G; Supplementary Fig. S2B and S2C). In contrast, knockout of A3A alone had no effect on basal or induced deaminase activity. This suggests that A3B is largely responsible for the increased deaminase activity in PC9 cells following EGFR inhibition although it is important to note that the oligonucleotide used in these assays is a better substrate for A3B than for A3A.

We next used a cellular competition assay to assess the functional effects of A3A/A3B knockout on the response of PC9 cells to EGFR inhibition. Although the majority of PC9 cells die in response to EGFR inhibition, a small population of cells survives treatment and persists as quiescent or slow-growing DTPs (refs. 48–50). Cells in the DTP state can undergo continued evolution to become fully drug resistant (49), and pathways that regulate DTP survival can promote or forestall therapy resistance (48). We therefore tested whether the induction of A3A and A3B following EGFR inhibition
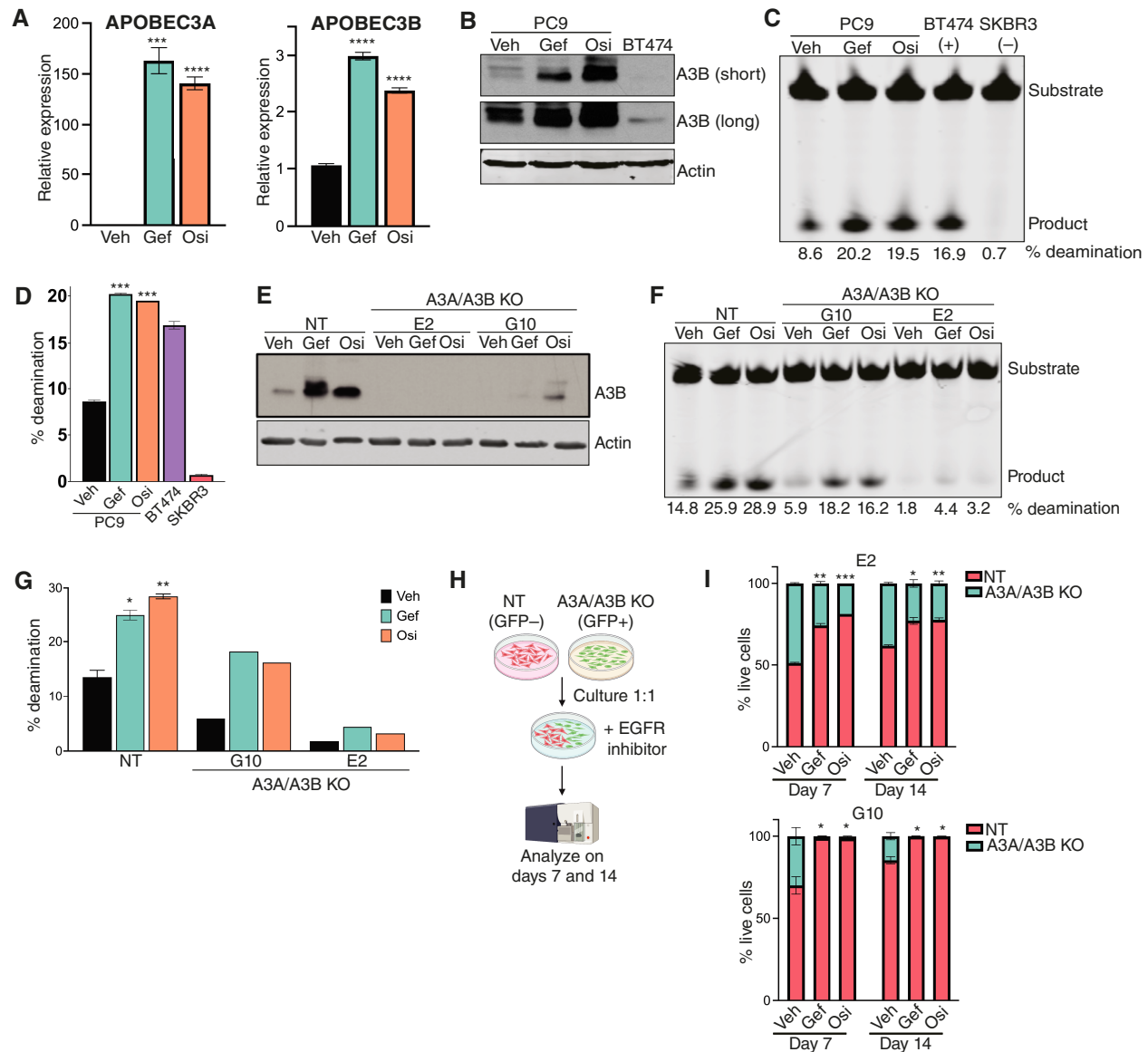
FIGURE 1 APOBEC3 activity is induced following EGFR inhibition. **A,** qRT-PCR analysis of a representative experiment showing A3A and A3B expression in PC9 cells following treatment with gefitinib or osimertinib for 24 hours. Error bars represent SEM of two biological replicates. Significance relative to the vehicle was determined using an unpaired t test. ***, $P < 0.0005$; ****, $P < 0.0001$. **B,** Western blots for A3B protein in PC9 cells following treatment with gefitinib or osimertinib for 24 hours. BT474 cells are shown as a positive control. Short and long exposures for A3B are shown. **C,** *In vitro* deaminase activity of PC9 cells treated with gefitinib or osimertinib for 24 hours. BT474 and SKBR3 cells are shown as positive and negative controls, respectively. % deamination was calculated as described in "Materials and Methods". **D,** Quantification of % deamination shown in **C**. Error bars represent SEM of two technical replicates. Significance relative to the vehicle was determined using an unpaired t test. ***, $P < 0.0005$. **E,** Western blots for A3B protein in PC9 cells expressing nontargeting gRNAs (NT) or gRNAs targeting both A3A and A3B (A3A/A3B KO). A pooled population is shown for NT cells, and two clones are shown for A3A/A3B-KO cells. Cells were treated with gefitinib or osimertinib for 24 hours. **F,** *In vitro* deaminase activity of PC9 cells expressing nontargeting gRNAs (NT) or gRNAs targeting both A3A and A3B (A3A/A3B KO). A pooled population is shown for NT cells, and two clones are shown A3A/A3B KO cells. Cells were treated with gefitinib or osimertinib for 24 hours, and % deamination was calculated as described in "Materials and Methods". **G,** Quantification of % deamination shown in **F**. Error bars represent SEM of two technical replicates. Significance relative to the NT vehicle was determined using an unpaired t test. *, $P < 0.05$; **, $P < 0.005$. **H,** Schematic of competition assay via flow cytometry. PC9 cells expressing nontargeting gRNAs (NT) or gRNAs targeting both A3A and A3B (A3A/A3B KO) were used for the experiment. **I,** Quantification of % live cells, either GFP negative or positive, after 7 or 14 days of EGFR inhibition. A pooled population is shown for NT cells and two clones are shown for A3A/A3B-KO cells. Error bars represent SEM of two biological replicates. An unpaired t test was used to determine statistical significance of GFP-positive cells in the treated condition relative to vehicle. *, $P < 0.05$; **, $P < 0.005$; ***, $P < 0.0005$. Gef, gefitinib; Osi, osimertinib; Veh, vehicle.

regulates the survival of DTPs. Control PC9 cells expressing a non-targeting sgRNA were mixed in a 1:1 ratio with GFP-labeled, A3A/A3B double-KO clones. Cells were then treated with vehicle, gefitinib, or osimertinib, and the proportion of GFP-positive cells was measured by flow cytometry after 7 and 14 days (Fig. 1H). In the absence of EGFR inhibitors, control and A3A/A3B-KO cells were present at approximately equal proportions although clone G10 had a slight competitive disadvantage (Fig. 1I). In contrast, A3A/A3B double-KO cells were markedly depleted starting just 7 days following EGFR inhibition and continuing through day 14 (Fig. 1I). These results suggest that the induction of A3A and A3B expression promotes the survival of DTPs following EGFR inhibition, corroborating previous findings (37, 38).

To determine whether induction of A3A or A3B plays a larger role in promoting DTP survival, we analyzed the behavior of A3A and A3B single-KO clones in a competition assay. Knockout of A3B alone led to a modest decrease in fitness following EGFR inhibition (Supplementary Fig. S2D). In contrast, the A3A-KO clone predicted to have complete knockout, B10, was significantly depleted following EGFR inhibition (Supplementary Fig. S2E). Interestingly, the A3A-KO clone predicted to have only a partial knockout of A3A, D3, did not have a competitive disadvantage following EGFR inhibition, suggesting that A3A expression may still be induced in this clone. To test this, we compared A3A induction following EGFR inhibition between control cells (NT) and each A3A-KO clone. Consistent with our prediction, we found that EGRF inhibition led to a robust induction of A3A in control cells and clone D3 but not in clone B10 (Supplementary Fig. S2F). Taken together, these results indicate that the complete knockout of A3A leads to a profound reduction in the survival of DTPs following EGFR inhibition, whereas knockout of A3B has only a modest effect.

Engineering an inducible system for APOBEC3B expression in PC9 cells

APOBEC mutagenesis is thought to occur in episodic bursts (51), and A3A and A3B expression in response to inflammatory stimuli is likewise transient (45). We therefore evaluated change in A3A and A3B expression during prolonged EGFR inhibition. A3A expression oscillated over 14 days (Fig. 2A). In contrast, A3B expression returned to baseline levels as early as 2 days following treatment with EGFR TKIs (Fig. 2A). Therefore, we next investigated the effects of sustained APOBEC activity on acquired resistance to EGFR inhibitors. To achieve this, we generated and characterized PC9 cells with a Cre recombinase–inducible A3B construct (Fig. 2B). Infection with adenovirus-expressing Cre led to a ~three-fold increase in A3B mRNA and protein expression (Fig. 2C and D) and a two-fold increase in deaminase activity (Fig. 2E and F). Importantly, this magnitude of increase in A3B expression and deaminase activity was similar to that observed following EGFR inhibition (cf. Fig. 1). Overexpression of A3B did not affect the growth or viability of PC9 cells in vitro (Fig. 2G). This system thus offers an opportunity to address the effects of sustained APOBEC3 activity on acquired therapy resistance.

APOBEC3B expression alters the evolutionary trajectory of acquired resistance to EGFR inhibitors

Using PC9 cells with conditional A3B expression, we examined the consequences of sustained A3B expression on acquired resistance to EGFR inhibitors. Five independent replicates of control cells (infected with GFP-expressing adenovirus; denoted as A3B-off A–E) and six independent replicates of A3B-expressing cells (Cre-infected; denoted as A3B-on A–F) were treated with 100 nmol/L gefitinib, and cells were passaged weekly until the cells grew consistently in the presence of drug. Aliquots of each replicate cell population not treated with gefitinib, denoted as gefitinib-sensitive, were saved for subsequent comparisons. Consistent with previous studies (49, 52), control PC9 cells evolved resistance to gefitinib over 1 to 4 months, with one subset of cells developing resistance at around 30 to 40 days and the other subset developing resistance at later timepoints ranging from 60 to 100 days (Fig. 3A). A3B-expressing cells developed resistance with the same kinetics as control cells, suggesting that sustained A3B expression does not alter the kinetics with which PC9 cells evolve resistance to gefitinib.

To further characterize each GR control and A3B-expressing population, we measured the concentration of gefitinib required to inhibit growth by 50% in both sensitive and GR cells (Fig. 3B; Supplementary Fig. S3A). The concentration required to inhibit growth by 50% for gefitinib in sensitive cells ranged from 10 to 20 nmol/L, as expected (49). In contrast, concentrations of gefitinib up to 1 μmol/L did not affect cell growth in GR cells. We calculated the AUC for the dose–response curves in sensitive and GR cells. As expected, in both A3B-off and A3B-on contexts, resistant cells had greater AUC values, confirming that GR cells are markedly resistant to gefitinib (Fig. 3C).

We repeated this resistance assay with an additional set of four control (A3B-off G, I–K) and five A3B-expressing cells (A3B-on G–K; Supplementary Fig. S4A). Similar to the previous experiment, we observed that PC9 cells, regardless of A3B expression, acquired resistance to a low dose of gefitinib within 100 days. Cells that did not acquire resistance within this timeframe (A3B-off H) were excluded from the dataset. We characterized these cells and confirmed that the GR cells were markedly resistant to gefitinib (Supplementary Fig. S4B) and that A3B activity is maintained in GR cells (Supplementary Fig. S4C).

We next evaluated the prevalence of the $EGFR^{T790M}$ mutation in sensitive and resistant cells (Fig. 3D and E; Supplementary Fig. S3B). $EGFR^{T790M}$ mutation was detected in two of five (40%) A3B-off GR cells (A3B-off GRD and GRE), consistent with previous findings (49, 53). Interestingly, both A3B-off GRD and GRE cells developed gefitinib resistance at early timepoints, consistent with previous studies suggesting that early gefitinib resistance arises from preexisting clones with $EGFR^{T790M}$ mutations (49). In contrast, five of six (83%) A3B-on GR cells had an $EGFR^{T790M}$ mutation (Fig. 3D and E). Of these, two A3B-expressing cell lines (A3B-on GRA and GRF) developed gefitinib resistance early, as expected. Unexpectedly, however, three A3B-expressing cell lines (A3B-on GRC, GRD, and GRE) with T790M mutations developed gefitinib resistance at late timepoints. This suggests that, in the presence of sustained A3B expression, $EGFR^{T790M}$ mutations are more likely to arise late during the evolution of therapy resistance.

Integrated genomic analysis of GR PC9 cells

To gain additional insights into the consequences of APOBEC activity on acquired gefitinib resistance, we performed genomic analyses of control and APOBEC3B-expressing cells, both in gefitinib-sensitive and GR contexts. Given the role of APOBEC3 enzymes in inducing mutations, we first used WES to assess the number of mutations present in the coding region of each cell line. We sequenced four control (A3B-off: GRA, GRC, GRD, and GRE)
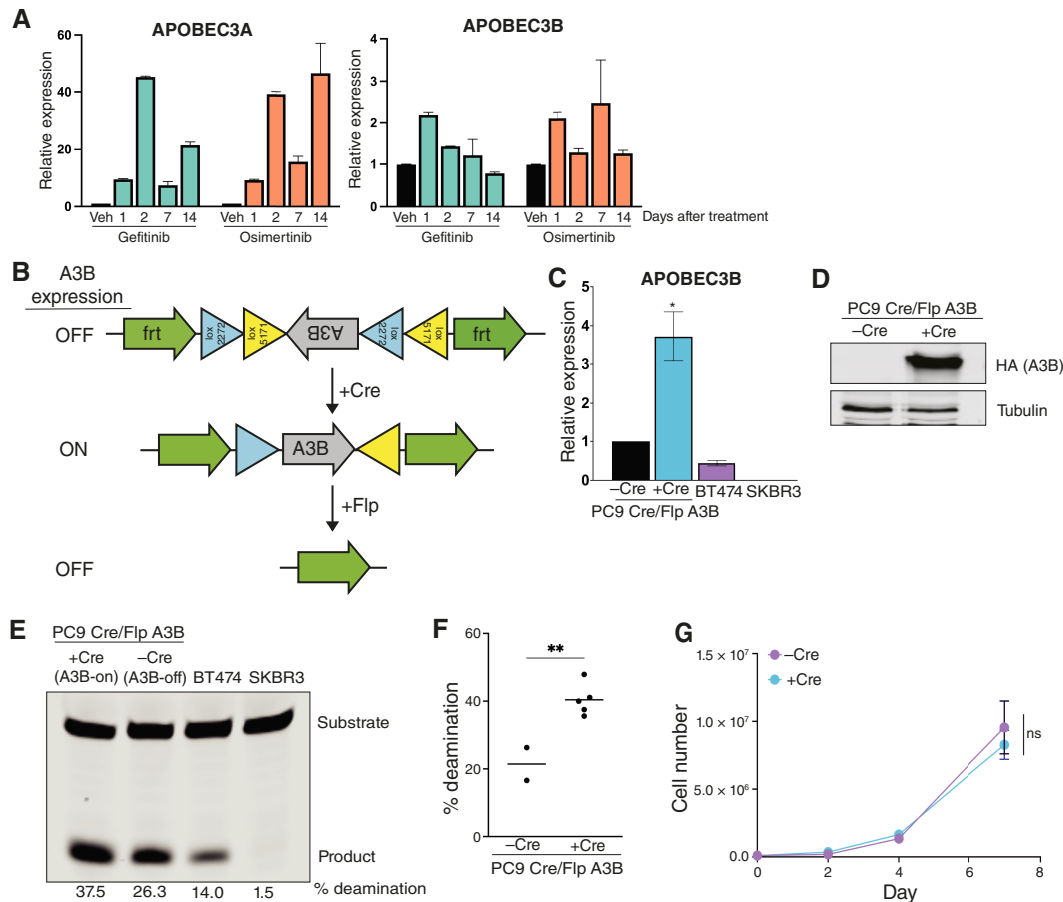
FIGURE 2 Engineering an inducible system for APOBEC3B expression in PC9 cells. **A,** qRT-PCR analysis showing A3A and A3B expression in PC9 cells following treatment with gefitinib or osimertinib over the course of 14 days. Error bars represent SEM of three technical replicates. Veh, vehicle. **B,** Schematic of Cre-inducible APOBEC3B expression. **C,** qRT-PCR analysis showing A3B expression in PC9 cells following infection with Cre recombinase. Error bars represent SEM of three technical replicates. *, $P < 0.05$. BT474 and SKBR3 cells are shown as controls. **D,** Western blots showing protein expression of HA-tagged A3B in PC9 cells following infection with Cre recombinase. **E,** *In vitro* deaminase activity assay in PC9 cells following infection with Cre recombinase. BT474 and SKBR3 cells are shown as controls. % deamination was calculated as described in "Materials and Methods". **F,** Quantification of % deamination in two replicates of control PC9 cells (−Cre) and five replicates of A3B-expressing PC9 (+Cre). % deamination was calculated as described in "Materials and Methods". An unpaired *t* test was performed to determine statistical significance. **, $P < 0.005$. **G,** Growth curves for PC9 cells expressing A3B (+Cre) or control cells (−Cre). Error bars represent SEM of two biological replicates. A two-way ANOVA was performed to determine statistical significance. ns, not significant.

and five A3B-expressing (A3B-on: GRA, GRB, GRC, GRD, and GRF) GR cells, along with corresponding gefitinib-sensitive control (A3B-off: A and B) and A3B-expressing (A3B-on: A, B, D, and F) cells. Finally, parental PC9 cells were sequenced as a reference, and mutations observed in parental PC9 cells were filtered out from subsequent analyses (see "Materials and Methods").

APOBEC3B expression in gefitinib-sensitive cells did not lead to an increase in the number of observed mutations (Fig. 4A; average mutations/exome: A3B-off, 10.5; A3B-on, nine), likely because APOBEC-induced mutations are distributed throughout the genome, and so in a population of cells, any individual mutation will be present at very low rates, below the limit of detection by next-generation sequencing (51). In contrast, the acquisition of gefitinib resistance

was associated with a marked increase in the number of mutations (Fig. 4A; average mutations/exome: A3B-off, 70.3; A3B-on, 90.4). Interestingly, A3B-on GR cells did not have significantly more mutations than A3B-off GR cells, suggesting that the increased number of mutations observed in GR cells was independent of ectopic A3B expression. There are several possible explanations for the increased mutational burden, including other mutagenic processes operative in these cells, the selection for preexisting subclones with distinct mutations, or the activity of endogenous A3A and A3B induced by gefitinib treatment. Consistent with this latter possibility, both A3B-off and A3B-on GR cells had an increase in C-to-T transitions and C-to-G transversions occurring in a TCW context, which is the APOBEC consensus motif (Supplementary File S1). Although the total number of mutations was too low to extract mutational signatures, the presence of these APOBEC consensus mutations in GR cells
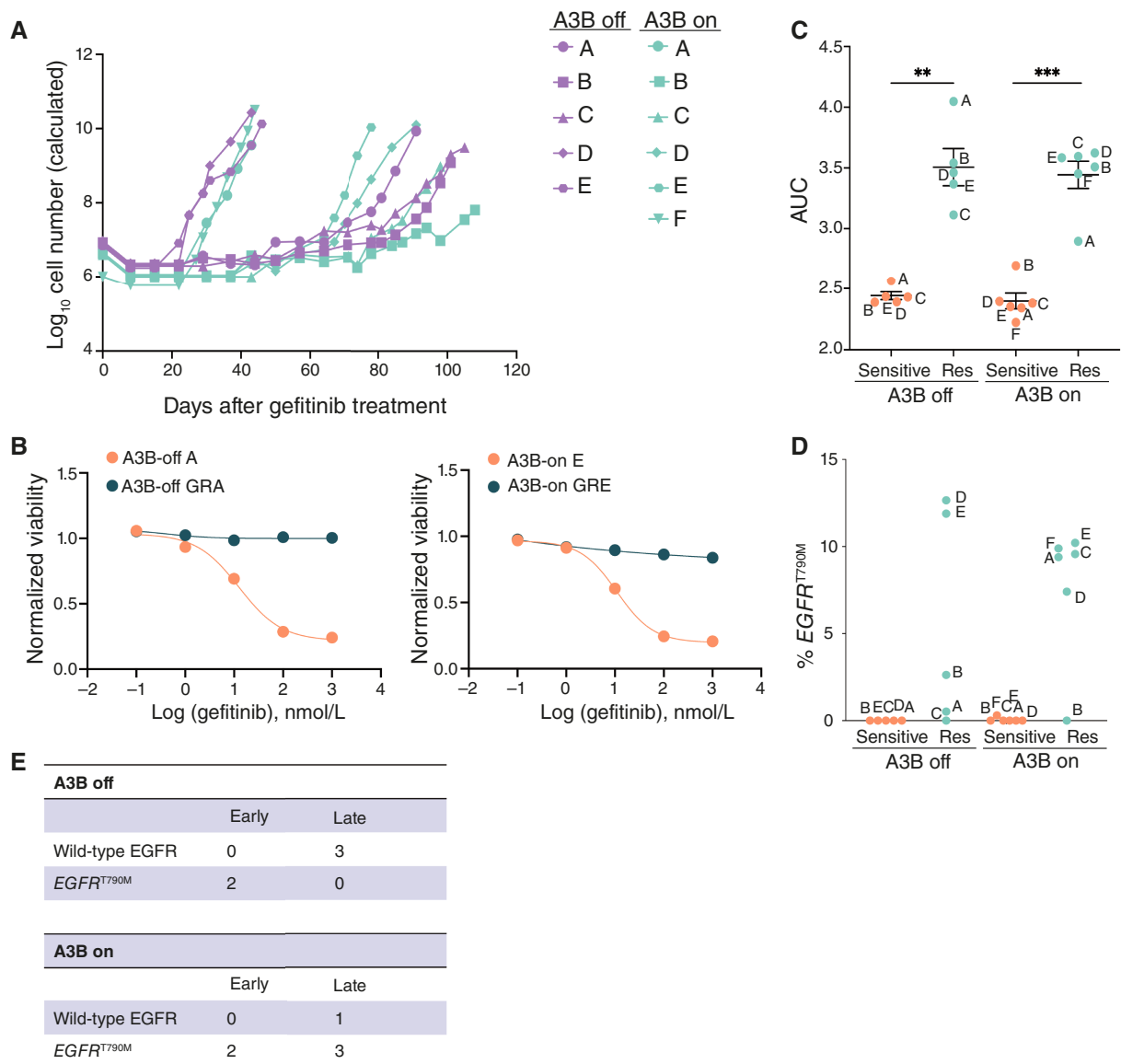
FIGURE 3 APOBEC3B expression alters the evolutionary trajectory of acquired resistance to EGFR inhibitors. **A,** Kinetics of evolution of gefitinib resistance in PC9 cells with or without A3B expression. **B,** Representative dose–response curves to gefitinib for sensitive and resistant A3B-off and A3B-on PC9 cells. **C,** Quantification of the AUC of dose–response curves for gefitinib-sensitive and GR A3B-off and A3B-on PC9 cells. An unpaired *t* test was performed to determine statistical significance. **, $P < 0.05$; ***, $P < 0.0005$. **D,** Frequency of $EGFR^{T790M}$ mutation as determined by droplet digital PCR in gefitinib-sensitive and GR A3B-off and A3B-on PC9 cells. % $EGFR^{T790M}$ was calculated as described in "Materials and Methods". **E,** Contingency tables summarizing the relationship between resistance kinetics and EGFR mutation status in A3B-off and A3B-on PC9 cells. Res, resistant.

suggests a contribution of endogenous APOBEC activity to the total mutational burden.

To identify potential genetic drivers of gefitinib resistance in these cells, we examined exome sequencing data for mutations in genes that are commonly mutated in lung adenocarcinoma (54), squamous carcinoma (55), or small cell cancer (56). We also analyzed genes that are differentially expressed between lung adenocarcinomas and small cell or squamous cell lung cancer (57–60). Combining these gene lists yielded 129 genes that are either significantly mutated in each lung cancer subtype or are differentially expressed

across subtypes (Supplementary Table S2). We used MuTect2 to identify mutations present in GR cells but not in parental PC9 cells. Importantly, a 15 bp deletion in exon 19 of EGFR and a homozygous R248Q mutation in p53 were detected in all cells, consistent with the presence of these mutations in parental PC9 cells (61). However, with the exception of $EGFR^{T790M}$ mutation (see above), only the *MGA* gene was mutated in multiple GR cells (A3B-off GRD and A3B-off GRE; Supplementary Table S3). Similarly, aside from $EGFR^{T790M}$, none of the known genetic mechanisms of resistance to EGFR inhibition was observed in these cells. Therefore, we reasoned that nongenetic mechanisms may be responsible for gefitinib
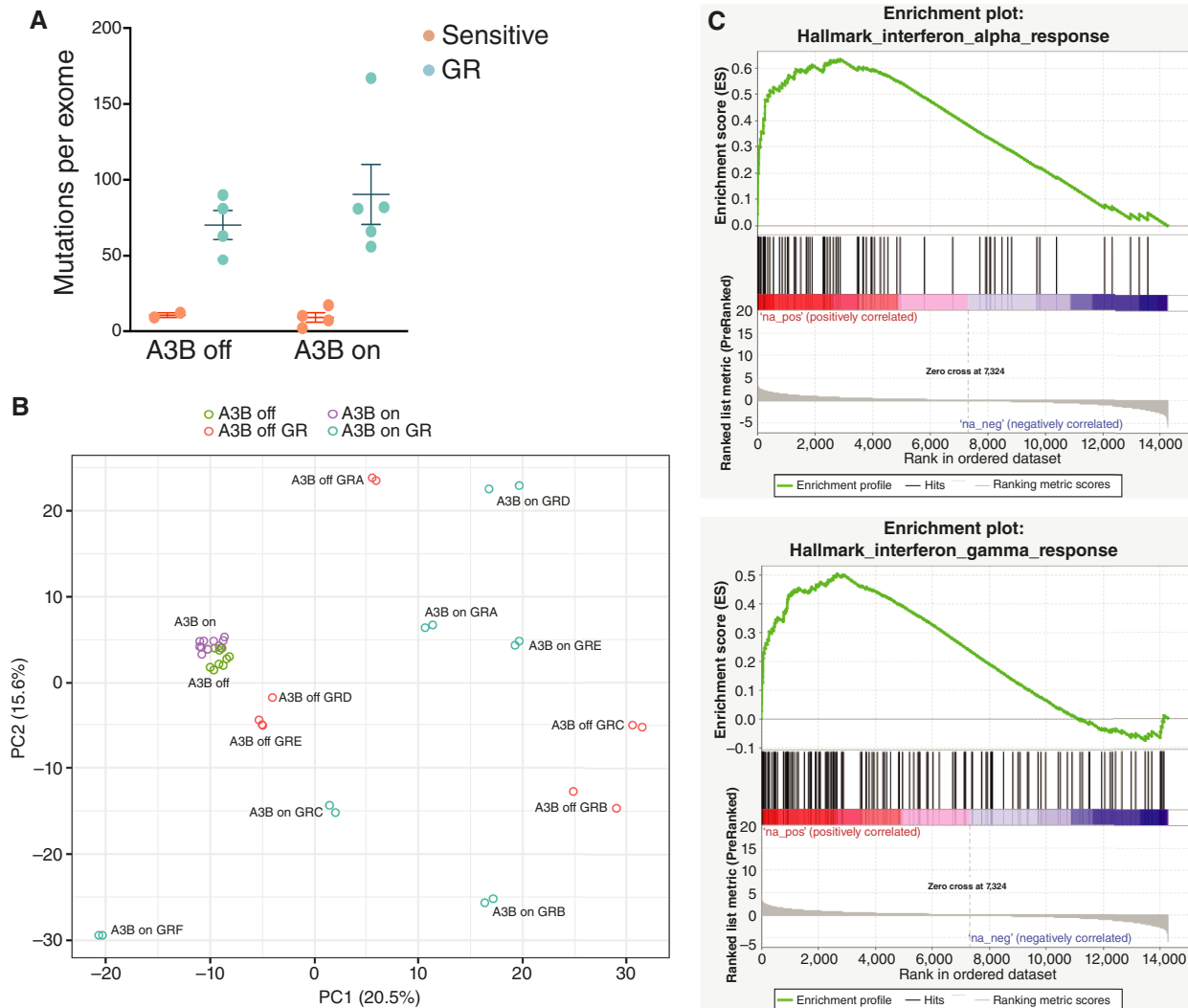
FIGURE 4 Integrated genomic analysis of GR PC9 cells. **A,** Quantification of mutations per exome in A3B-off and A3B-on GR cells. Mutations were called as described in "Materials and Methods". **B,** PCA from RNA-seq data. **C,** Gene set enrichment analysis comparing A3B-on and A3B-off sensitive PC9 cells.

resistance in these cells. To address this, we performed RNA-seq on all A3B-off and A3B-on cells. We first assessed the effect of A3B expression on gene expression in gefitinib-sensitive PC9 cells using RNA-seq. Principal components analysis (PCA) of control and A3B-expressing gefitinib-sensitive cells revealed that A3B expression led to modest but consistent changes in gene expression (Fig. 4B). Gene set enrichment analysis showed that A3B expression led to upregulation of pro-inflammatory gene expression programs, including IL6_JAK_STAT3_SIGNALING, INTERFERON_ALPHA_RESPONSE, and INTERFERON_GAMMA_RESPONSE (Fig. 4C; Supplementary File S2).

We next compared the transcriptional profiles of GR cells with and without A3B expression. We confirmed that A3B expression remains high in the GR cells (Supplementary Fig. S5A). A3B-off GR cells with a T790M mutation (A3B-off GRD and GRE) clustered near gefitinib-sensitive cells on a PCA plot, consistent with the notion that these cells have sustained EGFR

signaling and very similar gene expression profiles to gefitinib-sensitive cells (Fig. 4B). In contrast, A3B-off GR cells lacking the T790M mutation (A3B-off GRA, GRB, and GRC) were more distant on the PCA plot, suggesting these cells have distinct transcriptional profiles, possibly due to activation of different oncogenic programs in these cells (Fig. 4B). These results are also consistent with previous findings that PC9 cells that develop resistance early are transcriptionally more similar to parental PC9 cells, whereas PC9 cells that develop EGFR inhibitor resistance at late timepoints, via evolution in the DTP state, have distinct gene expression profiles (49).

We next examined the transcriptional profile of A3B-on GR cells. Interestingly, A3B-on GR cells had gene expression patterns that were distinct from both parental cells and from one another, irrespective of their T790M status (Fig. 4B). This is consistent with the possibility that A3B expression promotes the evolution of resistance during the DTP state, leading to GR cells with divergent transcriptional programs.

APOBEC3B-expressing PC9 cells show evidence of squamous cell transdifferentiation during acquired gefitinib resistance

We next examined RNA-seq data for evidence of nongenetic resistance mechanisms in GR cells. Given the relationship between APOBEC mutagenesis and histologic transformation, we first asked whether any GR cells had evidence of small cell or squamous cell transdifferentiation. None of the GR cells exhibited changes in expression of genes encoding the neuroendocrine markers synaptophysin or chromagranin, which are expressed in SCLC. Furthermore, expression of RB1, TP53, and MYC remained consistent between A3B-off and A3B-on sensitive and resistant cells (Supplementary Fig. S5B). A loss of both Rb and p53 and amplification of Myc are associated with small cell carcinoma histology (31, 62, 63). Together, these data suggest that gefitinib resistance in these cells is not associated with transdifferentiation to neuroendocrine SCLC.

We next examined the expression of the squamous cell transcription factor p63, which is essential for the development of squamous epithelium and highly expressed in squamous cell cancers, including squamous lung cancer (64, 65). RNA-seq data revealed that two A3B-on resistant cell lines – GRB and GRF – had high expression of p63 (Fig. 5A). In contrast, none of the five A3B-off resistant cell lines upregulated p63. qRT-PCR confirmed this finding and showed that total p63 and the oncogenic variant ΔNp63 were both higher in the resistant cells compared with the matched sensitive lines (Fig. 5B). IHC staining for ΔNp63 further validated that these GR cells have high p63 expression, both *in vitro* and when grown as xenograft tumors *in vivo* (Fig. 5D and E; Supplementary Fig. S6A).

To extend these data, we used qRT-PCR to analyze ΔNp63 expression in four additional A3B-off and five A3B-on GR lines (see Supplementary Fig. S4A). We found that one A3B-off (A3B-off GRG) and two A3B-on (A3B-on GRG and GRH) lines exhibited high expression of ΔNp63 (Supplementary Fig. S6B). In total, one of nine A3B-off and four of 11 A3B-on GR cell lines showed upregulation of ΔNp63, suggesting that upregulation of this transcription factor occurs more frequently during acquired resistance to gefitinib in cells with constitutive expression of A3B.

p63 is a known regulator of lineage plasticity in cancer cells (64, 66) and its expression is associated with SCC transdifferentiation (33). Consistent with this, we found that the adenocarcinoma marker, *MUC5B*, was downregulated in A3B-on GRB and GRF cells (Fig. 5C). Moreover, SCC marker, *KRT6A,* and p63 target genes, *IL1A* and *IL1B,* were upregulated in A3B-on cells with high ΔNp63 expression (Fig. 5C; Supplementary Fig. S6B). Taken together, these data suggest that A3B-on GRB and GRF cells transdifferentiated to a squamous cell phenotype during the acquisition of gefitinib resistance. Interestingly, GRF cells have a T790M mutation, whereas GRB cells do not (Fig. 3D); this mirrors the clinical findings that squamous cell transdifferentiation can occur in the presence or absence of T790M (67).

We next asked whether knockout of A3A and A3B prevents the acquisition of resistance through ΔNp63 upregulation. To address this, control or A3A/A3B-KO cells were treated with osimertinib and cells were passaged weekly until the acquisition of resistance (Supplementary Fig. S6C). Osimertinib-resistant cells were analyzed by qRT-PCR to assess ΔNp63 expression. We found that ΔNp63 was upregulated in three of five resistant cell lines derived from parental cells and two of four resistant cell lines derived from NT cells (Supplementary Fig. S6D). In contrast, zero of five resistant cell lines derived from A3A/A3B-KO cells had ΔNp63 upregulation (Supplementary Fig. S6D). Taken together with the results from PC9 cells with constitutive A3B expression, these results suggest that APOBEC3 activity contributes to squamous transdifferentiation during acquired resistance to EGFR inhibition.

p63 knockout reduces inflammatory gene expression and sensitizes PC9 GR cells to EGFR inhibition

To evaluate the function of ΔNp63 in GR cells we used A3B-on GRF cells as these expressed high levels of ΔNp63. We first measured sensitivity to osimertinib, a third-generation EGFR inhibitor effective against the T790M mutation. As controls we used two gefitinib-sensitive lines, A3B-on F and E, and the GR line A3B-on GRE, which has an $EGFR^{T790M}$ mutation but does not express ΔNp63. As expected, A3B-on GRE cells (IC50: 12.66 nmol/L) were sensitive to osimertinib, with IC_{50} values similar to the gefitinib-sensitive lines (A3B-on F, 17.48 nmol/L and A3B-on E, 14.11 nmol/L). In contrast, A3B-on GRF cells (IC_{50}, 81.97 nmol/L), which express ΔNp63, were more resistant to osimertinib treatment (Fig. 6A). To explore the molecular basis for this difference, we tested whether osimertinib effectively inhibited EGFR signaling in these cells. Although treatment with 100 nmol/L osimertinib completely abolished EGFR phosphorylation in gefitinib-sensitive and A3B-on GRE cells, this dose of drug only partially inhibited EGFR phosphorylation in A3B-on GRF (Fig. 6B).

To test whether high expression of ΔNp63 directly promotes osimertinib resistance in these cells, we knocked out the *TP63* gene using CRISPR/Cas9 (Fig. 6C). The expression of the ΔNp63 target genes *IL1A* and *IL1B* was reduced in p63-KO cells, confirming functional knockout (Fig. 6D). Although p63 knockout did not affect the growth of A3B-on GRF cells *in vitro* (Fig. 6E), its knockout sensitized these cells to osimertinib treatment over 3 and 6 days (Fig. 6F and G). A3B-on GRF cells expressing a control vector had an IC_{50} of 20.40 nmol/L, which was lower than the IC_{50} of parental A3B-on GRF cells (cf. Fig. 6A). Nonetheless, A3B-on GRF p63-KO 1 and -KO 3 cells had IC_{50}s of 9.89 and 15.60 nmol/L, respectively. These findings show that high expression of ΔNp63 in GR cells with a T790M mutation promotes resistance to third-generation EGFR inhibitors in these cells. To explore the mechanistic basis for this resistance, we examined the expression of EGFR ligands as increased expression of these ligands promotes resistance to EGFR inhibition (68–72). We found that the expression of amphiregulin (*AREG*) and epiregulin (*EREG*) was increased in A3B-on GRF cells (Supplementary Fig. S6E). Furthermore, this increase was dependent on ΔNp63 as knockout of p63 blunted both *AREG* and *EREG* expression (Supplementary Fig. S6F). This suggests that ΔNp63 promotes resistance to EGFR inhibition in part through upregulation of EGFR ligands.

Finally, to extend these results to humans, we examined the expression of the APOBEC3 genes (A3A and A3B), various adenocarcinoma (NKX2-1 and MUC5B) and squamous (TP63 and SOX2) markers, and the inflammatory genes *IL1A* and *IL1B* in published gene expression datasets from patients with lung cancer with an adenocarcinoma or squamous cell histology (73).
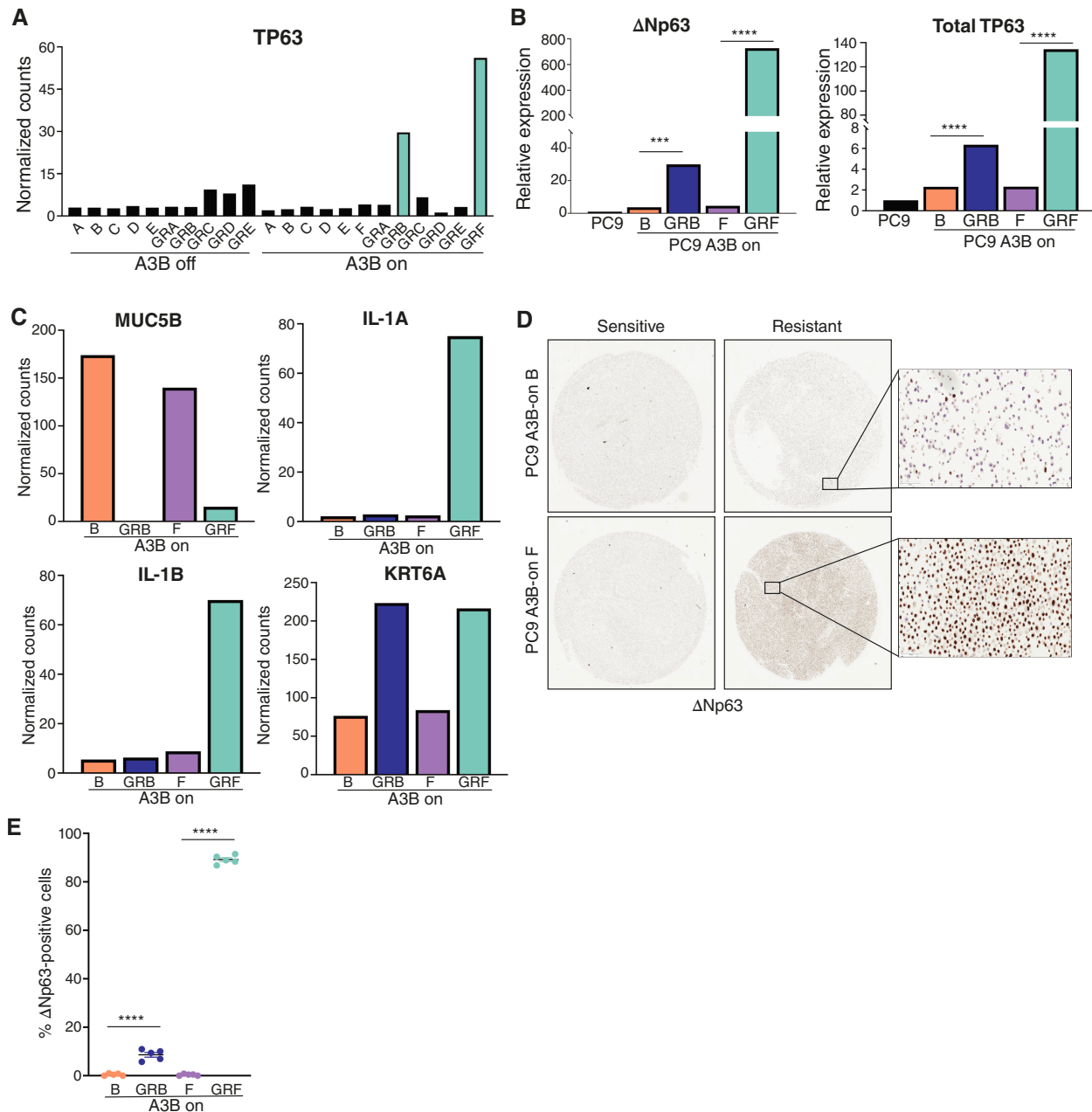
FIGURE 5 APOBEC3B-expressing PC9 cells show evidence of squamous cell transdifferentiation during acquired gefitinib resistance. **A,** Normalized gene counts for TP63 from RNA-seq in gefitinib-sensitive and GR PC9 cells, with or without A3B expression. **B,** qRT-PCR analysis showing ΔNp63 and total p63 mRNA expression in gefitinib-sensitive and GR PC9 A3B-on cells. Parental PC9 are shown as a control. Error bars represent SEM of three technical replicates. An unpaired t test was performed to determine statistical significance. ***, $P < 0.0005$; ****, $P < 0.0001$. **C,** Normalized gene counts for MUC5B, IL-1A, IL-1B, and KRT6A from RNA-seq in gefitinib-sensitive and GR PC9 cells expressing A3B. **D,** IHC images showing ΔNp63 protein expression in sensitive and resistant PC9 A3B-on cells. Insets are shown at 20× magnification. **E,** Quantification of ΔNp63-positive cells for sensitive and resistant PC9 A3B-on cells shown in **D**. Each point represents a field of view at 20× magnification. Error bars represent SEM of five fields of view. An unpaired t test was performed to determine statistical significance. ***, $P < 0.0005$; ****, $P < 0.0001$.

We found that the expression of A3A, A3B, and IL1A was modestly elevated (1.4–1.7-fold) in squamous cancers as compared with adenocarcinomas (Supplementary Fig. S7A–S7E). Consistent with this, the expression of A3A – and to a lesser extent A3B, IL1A, and IL1B – was correlated with the squamous markers but not the adenocarcinoma markers in this dataset (Supplementary Fig. S7F). These clinical data support our mechanistic findings linking APOBEC activity to squamous transdifferentiation and inflammatory gene expression.
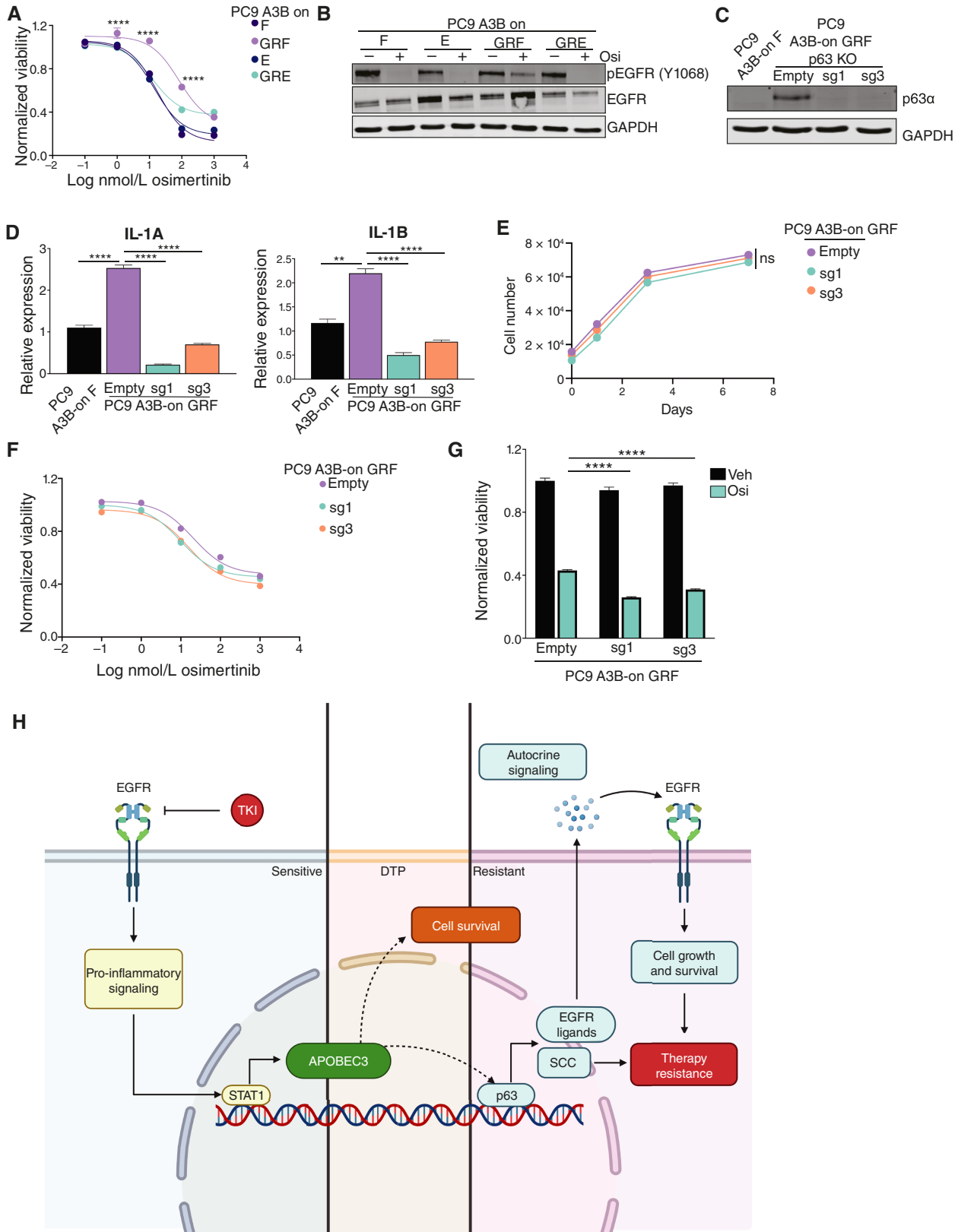
FIGURE 6 p63 knockout reduces inflammatory gene expression and sensitizes PC9 GR cells to EGFR inhibition. **A,** Dose–response curve of osimertinib in gefitinib-sensitive and GR PC9 cells expressing A3B. Viability was measured using CellTiter Glo following 3 days of drug treatment. A two-way ANOVA with the Tukey multiple comparisons test was used to determine statistical significance at *(Continued on the following page.)*

(*Continued*) each dose. ****, *P* < 0.0001 when comparing PC9 A3B-on GRF and GRE cells at the indicated dose. **B,** Western blots for pEGFR (Y1068) and total EGFR in gefitinib-sensitive and GR PC9 cells expressing A3B. Cells were treated with osimertinib (Osi) for 24 hours. **C,** Western blots for p63α in PC9 A3B-on GRF cells expressing an empty vector or gRNAs targeting p63 (sg1 and sg3). PC9 A3B-on F cells are shown as a control. **D,** qRT-PCR analysis showing IL-1A and IL-1B expression in PC9 A3B-on GRF cells expressing an empty vector or gRNAs targeting p63 (sg1 and sg3). PC9 A3B-on F cells are shown as a control. Error bars represent SEM of three technical replicates. An unpaired *t* test was performed to determine statistical significance. **, *P* < 0.005; ****, *P* < 0.0001. **E,** *In vitro* growth curves of PC9 A3B-on GRF cells with or without p63 knockout. A two-way ANOVA was performed to determine statistical significance. ns, not significant. **F,** Dose–response curve of osimertinib in PC9 A3B-on GRF cells expressing an empty vector or gRNAs targeting p63 (sg1 and sg3). Viability was measured using CellTiter Glo following 3 days of drug treatment. A two-way ANOVA was performed, which determined a significant p63 status × dose interaction with a *P* value of 0.02. **G,** Viability of PC9 A3B-on GRF cells expressing an empty vector or gRNAs targeting p63 (sg1 and sg3) following treatment with osimertinib for 6 days. A two-way ANOVA with the Dunnett test was performed to determine statistical significance. ****, *P* < 0.00001. **H,** Model for the function of APOBEC3 in the survival and evolution of DTP cells during acquired resistance to EGFR inhibition. EGFR inhibition leads to STAT1-dependent upregulation of A3A and A3B. The expression of A3A and A3B is required for the survival of DTPs and is associated with an increased frequency of ΔNp63 upregulaiton and squamous transdifferentiation in the drug-resistant state. ΔNp63 expression in drug-resistant cells promotes osimertinib resistance in part through upregulation of EGFR ligands.

Discussion

TKIs that target EGFR are the current standard of care for patients with EGFR-mutant lung adenocarcinomas. Although these treatments are initially effective, resistance to TKIs occurs within months (18–20). Understanding the mechanisms that can lead to acquired drug resistance can provide better insights into the treatment of this subset of patients.

In the current study, we examined the regulation and functional consequences of APOBEC3 activity during acquired resistance to EGFR inhibition (Fig. 6H). We show that targeted therapies against EGFR induce APOBEC activity in an EGFR-mutant NSCLC cell line. EGFR inhibition leads to a transient increase in A3A and A3B expression and APOBEC deaminase activity. This mirrors clinical data that show an increase in the APOBEC mutational signature in tumors from patients who have acquired resistance to an EGFR inhibitor, especially those with tumors that have undergone histologic transformation (34–36). Although sustained APOBEC activity does not accelerate acquired therapy resistance, A3B expression alters the evolutionary path that PC9 cells take to become gefitinib resistant. Specifically, A3B expression is associated with the late acquisition of T790M mutations during the DTP state. Consistent with this, knockout of A3A and A3B impairs the survival of DTPs, with A3A knockout having a more profound effect. It is important to note that our results do not imply that APOBEC3 activity directly induces the T790M mutation. Rather, these data support a model in which induction of APOBEC activity promotes DTP survival, thereby facilitating the on-going evolution of DTP cells. Importantly, these results corroborate recent findings from other groups demonstrating a role for therapy-induced APOBEC3 expression in DTP survival and therapy resistance in cell lines, PDX models, and patients (37, 38).

A subset of GR cells displays ΔNp63 upregulation and evidence of squamous cell transdifferentiation; importantly, ΔNp63 upregulation was more common in GR cells expressing A3B than in control cells. Consistent with this, knockout of A3A and A3B prevented ΔNp63 upregulation in osimertinib-resistant cells. This suggests that APOBEC activity may be functionally linked to this form of histologic transformation. p63 is a p53 family member known for its role in maintaining stemness of epithelial cells (66, 74). Work from other labs has demonstrated that p63 amplification and, in turn, transcription of its target genes promotes cancer development and progression (64, 65, 75). Our findings suggest that ΔNp63 contributes to TKI resistance in squamous transdifferentiated lung cancer cells as knockout of p63 sensitized these cells to third-generation EGFR inhibitors, like osimertinib. We found that ΔNp63 regulates expression of EGFR ligands amphiregulin and epiregulin, suggesting a mechanism by which ΔNp63 may promote osimertinib resistance. These data may explain the clinical observation that lung cancers exhibiting transdifferentiation have a particularly poor prognosis. Furthermore, these findings may suggest avenues for future therapies. The use of ΔNp63 expression as a biomarker, for example, may predict whether a patient will respond to third-generation EGFR inhibitors. Therapies against ΔNp63 targets, such as IL-1α/β or EGFR ligands, may also prove useful in the clinical setting. Interestingly, we observed ΔNp63 upregulation in GR cells both with and without the $EGFR^{T790M}$ mutation, suggesting that these resistance mechanisms can co-occur, consistent with clinical observations (76–83).

In conclusion, our findings provide mechanistic insights into the link between APOBEC mutagenesis, TKI resistance, and histologic transformation in EGFR-mutant lung cancer. More broadly, our work identifies a role for APOBEC3 induction in promoting the survival of DTPs following oncogene-targeted therapies. Future work will define whether APOBEC3 induction is a common response to diverse targeted therapies and whether APOBEC-dependent survival of DTPs can promote therapy resistance across different tumor types. In addition, elucidating the mechanistic links between APOBEC3 activity and ΔNp63 upregulation will shed light on the relationship between this important mutagenic processes and histologic transformation.

Limitations of the study

There are several limitations to our study. First, the Cre-inducible model used here leads to sustained APOBEC3B expression, but previous studies suggest that APOBEC3 mutagenesis occurs in episodic bursts. It is possible that the functional consequences of sustained versus episodic APOBEC3 activity are distinct. Second, we did not conduct an extensive analysis of the drug-tolerant state. In future work, it will be important to dissect subclonal heterogeneity, and define the timing and frequency of ΔNp63 upregulation, within DTPs. Third, in order to achieve complete knockout of A3A or A3B,

we used single-cell clones for these experiments; it will be important to confirm our findings using polyclonal populations of cells.

Authors' Disclosures

Authors' Contributions

N.M.G. Garcia: Conceptualization, data curation, investigation, writing–original draft. **J.N. Becerra:** Conceptualization, data curation, investigation, writing–original draft. **S. Srinivasan:** Data curation, validation, investigation. **B.J. McKinney:** Data curation, investigation. **A.V. DiMarco:** Conceptualization, data curation, investigation. **F. Wu:** Data curation, formal analysis, methodology. **M. Fitzgibbon:** Data curation, software, formal analysis, investigation, methodology. **J.V. Alvarez:** Conceptualization, resources, formal analysis, supervision, funding acquisition, validation, investigation, writing–original draft, writing–review and editing.

Acknowledgments

Note

Supplementary data for this article are available at Cancer Research Communications Online (https://aacrjournals.org/cancerrescommun/).

References

1. Nik-Zainal S, Morganella S. Mutational signatures in breast cancer: the problem at the DNA level. Clin Cancer Res 2017;23:2617–29.

2. Alexandrov LB, Nik-Zainal S, Wedge DC, Campbell PJ, Stratton MR. Deciphering signatures of mutational processes operative in human cancer. Cell Rep 2013;3:246–59.

3. Helleday T, Eshtad S, Nik-Zainal S. Mechanisms underlying mutational signatures in human cancers. Nat Rev Genet 2014;15:585–98.

4. Alexandrov LB, Nik-Zainal S, Wedge DC, Aparicio SAJR, Behjati S, Biankin AV, et al. Signatures of mutational processes in human cancer. Nature 2013;500:415–21.

5. Jamal-Hanjani M, Wilson GA, McGranahan N, Birkbak NJ, Watkins TBK, Veeriah S, et al. Tracking the evolution of non-small-cell lung cancer. N Engl J Med 2017;376:2109–21.

6. Burns MB, Lackey L, Carpenter MA, Rathore A, Land AM, Leonard B, et al. APOBEC3B is an enzymatic source of mutation in breast cancer. Nature 2013;494:366–70.

7. Law EK, Levin-Klein R, Jarvis MC, Kim H, Argyris PP, Carpenter MA, et al. APOBEC3A catalyzes mutation and drives carcinogenesis in vivo. J Exp Med 2020;217:e20200261.

8. Burns MB, Temiz NA, Harris RS. Evidence for APOBEC3B mutagenesis in multiple human cancers. Nat Genet 2013;45:977–83.

9. Petljak M, Dananberg A, Chu K, Bergstrom EN, Striepen J, von Morgen P, et al. Mechanisms of APOBEC3 mutagenesis in human cancer cells. Nature 2022;607:799–807.

10. Yan S, He F, Gao B, Wu H, Li M, Huang L, et al. Increased APOBEC3B predicts worse outcomes in lung cancer: a comprehensive retrospective study. J Cancer 2016;7:618–25.

11. Sieuwerts AM, Schrijver WAME, Dalm SU, de Weerd V, Moelans CB, Ter Hoeve N, et al. Progressive APOBEC3B mRNA expression in distant breast cancer metastases. PLoS One 2017;12:e0171343.

12. Law EK, Sieuwerts AM, LaPara K, Leonard B, Starrett GJ, Molan AM, et al. The DNA cytosine deaminase APOBEC3B promotes tamoxifen resistance in ER-positive breast cancer. Sci Adv 2016;2:e1601737.

13. Roper N, Gao S, Maity TK, Banday AR, Zhang X, Venugopalan A, et al. APOBEC mutagenesis and copy-number alterations are drivers of proteogenomic tumor evolution and heterogeneity in metastatic thoracic tumors. Cell Rep 2019;26:2651–66.e6.

14. Venkatesan S, Angelova M, Puttick C, Zhai H, Caswell DR, Lu W-T, et al. Induction of APOBEC3 exacerbates DNA replication stress and chromosomal instability in early breast and lung cancer evolution. Cancer Discov 2021;11:2456–73.

15. Lynch TJ, Bell DW, Sordella R, Gurubhagavatula S, Okimoto RA, Brannigan BW, et al. Activating mutations in the epidermal growth factor receptor underlying responsiveness of non-small-cell lung cancer to gefitinib. N Engl J Med 2004;350:2129–39.

16. Paez JG, Jänne PA, Lee JC, Tracy S, Greulich H, Gabriel S, et al. EGFR mutations in lung cancer: correlation with clinical response to gefitinib therapy. Science 2004;304:1497–500.

17. Pao W, Miller V, Zakowski M, Doherty J, Politi K, Sarkaria I, et al. EGF receptor gene mutations are common in lung cancers from "never smokers" and are associated with sensitivity of tumors to gefitinib and erlotinib. Proc Natl Acad Sci USA 2004;101:13306–11.

18. Mok TS, Wu Y-L, Thongprasert S, Yang C-H, Chu D-T, Saijo N, et al. Gefitinib or carboplatin-paclitaxel in pulmonary adenocarcinoma. N Engl J Med 2009;361:947–57.

19. Mitsudomi T, Morita S, Yatabe Y, Negoro S, Okamoto I, Tsurutani J, et al. Gefitinib versus cisplatin plus docetaxel in patients with non-small-cell lung cancer harbouring mutations of the epidermal growth factor receptor (WJTOG3405): an open label, randomised phase 3 trial. Lancet Oncol 2010;11:121–8.

20. Maemondo M, Inoue A, Kobayashi K, Sugawara S, Oizumi S, Isobe H, et al. Gefitinib or chemotherapy for non-small-cell lung cancer with mutated EGFR. N Engl J Med 2010;362:2380–8.

21. Del Re M, Tiseo M, Bordi P, D'Incecco A, Camerini A, Petrini I, et al. Contribution of KRAS mutations and c.2369C > T (p.T790M) EGFR to acquired resistance to EGFR-TKIs in EGFR mutant NSCLC: a study on circulating tumor DNA. Oncotarget 2017;8:13611–9.

22. Shih J-Y, Gow C-H, Yang P-C. EGFR mutation conferring primary resistance to gefitinib in non-small-cell lung cancer. N Engl J Med 2005;353:207–8.

23. Cross DAE, Ashton SE, Ghiorghiu S, Eberlein C, Nebhan CA, Spitzler PJ, et al. AZD9291, an irreversible EGFR TKI, overcomes T790M-mediated resistance to EGFR inhibitors in lung cancer. Cancer Discov 2014;4:1046–61.

24. Bean J, Brennan C, Shih J-Y, Riely G, Viale A, Wang L, et al. MET amplification occurs with or without T790M mutations in EGFR mutant lung tumors with acquired resistance to gefitinib or erlotinib. Proc Natl Acad Sci USA 2007;104:20932–7.

25. Engelman JA, Zejnullahu K, Mitsudomi T, Song Y, Hyland C, Park JO, et al. MET amplification leads to gefitinib resistance in lung cancer by activating ERBB3 signaling. Science 2007;316:1039–43.

26. Crystal AS, Shaw AT, Sequist LV, Friboulet L, Niederst MJ, Lockerman EL, et al. Patient-derived models of acquired resistance can identify effective drug combinations for cancer. Science 2014;346:1480–6.

27. Yu HA, Arcila ME, Rekhtman N, Sima CS, Zakowski MF, Pao W, et al. Analysis of tumor specimens at the time of acquired resistance to EGFR-TKI therapy in 155 patients with EGFR-mutant lung cancers. Clin Cancer Res 2013;19:2240–7.

28. Chung J-H, Rho JK, Xu X, Lee JS, Yoon HI, Lee CT, et al. Clinical and molecular evidences of epithelial to mesenchymal transition in acquired resistance to EGFR-TKIs. Lung Cancer 2011;73:176–82.

29. Weng C-H, Chen L-Y, Lin Y-C, Shih J-Y, Lin Y-C, Tseng R-Y, et al. Epithelial-mesenchymal transition (EMT) beyond EGFR mutations per se is a common mechanism for acquired resistance to EGFR TKI. Oncogene 2019;38:455–68.

30. Zhu X, Chen L, Liu L, Niu X. EMT-mediated acquired EGFR-TKI resistance in NSCLC: mechanisms and strategies. Front Oncol 2019;9:1044.

31. Oser MG, Niederst MJ, Sequist LV, Engelman JA. Transformation from non-small-cell lung cancer to small-cell lung cancer: molecular drivers and cells of origin. Lancet Oncol 2015;16:e165–72.

32. Shaurova T, Zhang L, Goodrich DW, Hershberger PA. Understanding lineage plasticity as a path to targeted therapy failure in EGFR-mutant non-small cell lung cancer. Front Genet 2020;11:281.

33. Hou S, Zhou S, Qin Z, Yang L, Han X, Yao S, et al. Evidence, mechanism, and clinical relevance of the transdifferentiation from lung adenocarcinoma to squamous cell carcinoma. Am J Pathol 2017;187:954–62.

34. Selenica P, Marra A, Choudhury NJ, Gazzo A, Falcon CJ, Patel J, et al. APOBEC mutagenesis, kataegis, chromothripsis in EGFR-mutant osimertinib-resistant lung adenocarcinomas. Ann Oncol 2022;33:1284–95.

35. Zhong J, Li X, Wang Z, Duan J, Li W, Zhuo M, et al. Evolution and genotypic characteristics of small cell lung cancer transformation in non-small cell lung carcinomas. J Natl Cancer Cent 2021;1:153–62.

36. Lee J-K, Lee J, Kim S, Kim S, Youk J, Park S, et al. Clonal history and genetic predictors of transformation into small-cell carcinomas from lung adenocarcinomas. J Clin Oncol 2017;35:3065–74.

37. Caswell DR, Gui P, Mayekar MK, Law EK, Pich O, Bailey C, et al. The role of APOBEC3B in lung tumor evolution and targeted cancer therapy resistance. Nat Genet 2024;56:60–73.

38. Isozaki H, Sakhtemani R, Abbasi A, Nikpour N, Stanzione M, Oh S, et al. Therapy-induced APOBEC3A drives evolution of persistent cancer cells. Nature 2023;620:393–401.

39. DiMarco AV, Qin X, McKinney BJ, Garcia NMG, Van Alsten SC, Mendes EA, et al. APOBEC mutagenesis inhibits breast cancer growth through induction of T cell-mediated antitumor immune responses. Cancer Immunol Res 2022;10:70–86.

40. Robles-Oteiza C, Taylor S, Yates T, Cicchini M, Lauderback B, Cashman CR, et al. Recombinase-based conditional and reversible gene regulation via XTR alleles. Nat Commun 2015;6:8783.

41. Akre MK, Starrett GJ, Quist JS, Temiz NA, Carpenter MA, Tutt ANJ, et al. Mutation processes in 293-based clones overexpressing the DNA cytosine deaminase APOBEC3B. PLoS One 2016;11:e0155391.

42. Maruyama W, Shirakawa K, Matsui H, Matsumoto T, Yamazaki H, Sarca AD, et al. Classical NF-κB pathway is responsible for APOBEC3B expression in cancer cells. Biochem Biophys Res Commun 2016;478:1466–71.

43. Leonard B, McCann JL, Starrett GJ, Kosyakovsky L, Luengas EM, Molan AM, et al. The PKC/NF-κB signaling pathway induces APOBEC3B expression in multiple human cancers. Cancer Res 2015;75:4538–47.

44. Periyasamy M, Singh AK, Gemma C, Farzan R, Allsopp RC, Shaw JA, et al. Induction of APOBEC3B expression by chemotherapy drugs is mediated by DNA-PK-directed activation of NF-κB. Oncogene 2021;40:1077–90.

45. Oh S, Bournique E, Bowen D, Jalili P, Sanchez A, Ward I, et al. Genotoxic stress and viral infection induce transient expression of APOBEC3A and pro-inflammatory genes through two distinct pathways. Nat Commun 2021;12:4917.

46. Xia Y, Stadler D, Lucifora J, Reisinger F, Webb D, Hösel M, et al. Interferon-γ and tumor necrosis factor-α produced by T cells reduce the HBV persistence form, cccDNA, without cytolysis. Gastroenterology 2016;150:194–205.

47. Mehta HV, Jones PH, Weiss JP, Okeoma CM. IFN-α and lipopolysaccharide upregulate APOBEC3 mRNA through different signaling pathways. J Immunol 2012;189:4088–103.

48. Oren Y, Tsabar M, Cuoco MS, Amir-Zilberstein L, Cabanos HF, Hütter J-C, et al. Cycling cancer persister cells arise from lineages with distinct programs. Nature 2021;596:576–82.

49. Hata AN, Niederst MJ, Archibald HL, Gomez-Caraballo M, Siddiqui FM, Mulvey HE, et al. Tumor cells can follow distinct evolutionary paths to become resistant to epidermal growth factor receptor inhibition. Nat Med 2016;22:262–9.

50. Sharma SV, Lee DY, Li B, Quinlan MP, Takahashi F, Maheswaran S, et al. A chromatin-mediated reversible drug-tolerant state in cancer cell subpopulations. Cell 2010;141:69–80.

51. Petljak M, Alexandrov LB, Brammeld JS, Price S, Wedge DC, Grossmann S, et al. Characterizing mutational signatures in human cancer cell lines reveals episodic APOBEC mutagenesis. Cell 2019;176:1282–94.e20.

52. Ogino A, Kitao H, Hirano S, Uchida A, Ishiai M, Kozuki T, et al. Emergence of epidermal growth factor receptor T790M mutation during chronic exposure to gefitinib in a non small cell lung cancer cell line. Cancer Res 2007;67:7807–14.

53. Sequist LV, Waltman BA, Dias-Santagata D, Digumarthy S, Turke AB, Fidias P, et al. Genotypic and histological evolution of lung cancers acquiring resistance to EGFR inhibitors. Sci Transl Med 2011;3:75ra26.

54. Cancer Genome Atlas Research Network. Comprehensive molecular profiling of lung adenocarcinoma. Nature 2014;511:543–50.

55. Cancer Genome Atlas Research Network. Comprehensive genomic characterization of squamous cell lung cancers. Nature 2012;489:519–25.

56. George J, Lim JS, Jang SJ, Cun Y, Ozretić L, Kong G, et al. Comprehensive genomic profiles of small cell lung cancer. Nature 2015;524:47–53.

57. Shriwash N, Singh P, Arora S, Ali SM, Ali S, Dohare R. Identification of differentially expressed genes in small and non-small cell lung cancer based on meta-analysis of mRNA. Heliyon 2019;5:e01707.

58. Long F, Su J-H, Liang B, Su L-L, Jiang S-J. Identification of gene biomarkers for distinguishing small-cell lung cancer from non-small-cell lung cancer using a network-based approach. Biomed Res Int 2015;2015:685303.

59. Lin EW, Karakasheva TA, Lee D-J, Lee J-S, Long Q, Bass AJ, et al. Comparative transcriptomes of adenocarcinomas and squamous cell carcinomas reveal molecular similarities that span classical anatomic boundaries. PLoS Genet 2017;13:e1006938.

60. Yuan F, Lu L, Zou Q. Analysis of gene expression profiles of lung cancer subtypes with machine learning algorithms. Biochim Biophys Acta Mol Basis Dis 2020;1866:165822.

61. Berger AH, Brooks AN, Wu X, Shrestha Y, Chouinard C, Piccioni F, et al. High-throughput phenotyping of lung cancer somatic mutations. Cancer Cell 2017;32:884.

62. Wang W, Xu C, Chen H, Jia J, Wang L, Feng H, et al. Genomic alterations and clinical outcomes in patients with lung adenocarcinoma with transformation to small cell lung cancer after treatment with EGFR tyrosine kinase inhibitors: a multicenter retrospective study. Lung Cancer 2021;155:20–7.

63. Offin M, Chan JM, Tenet M, Rizvi HA, Shen R, Riely GJ, et al. Concurrent RB1 and TP53 alterations define a subset of EGFR-mutant lung cancers at risk for histologic transformation and inferior clinical outcomes. J Thorac Oncol 2019;14:1784–93.

64. Massion PP, Taflan PM, Jamshedur Rahman SM, Yildiz P, Shyr Y, Edgerton ME, et al. Significance of p63 amplification and overexpression in lung cancer development and prognosis. Cancer Res 2003;63:7113–21.

65. Moses MA, George AL, Sakakibara N, Mahmood K, Ponnamperuma RM, King KE, et al. Molecular mechanisms of p63-mediated squamous cancer pathogenesis. Int J Mol Sci 2019;20:3590.

66. Melino G, Memmi EM, Pelicci PG, Bernassola F. Maintaining epithelial stemness with p63. Sci Signal 2015;8:re9.

67. Perez-Moreno P, Brambilla E, Thomas R, Soria J-C. Squamous cell carcinoma of the lung: molecular subtypes and therapeutic opportunities. Clin Cancer Res 2012;18:2443–51.

68. Ma S, Zhang L, Ren Y, Dai W, Chen T, Luo L, et al. Epiregulin confers EGFR-TKI resistance via EGFR/ErbB2 heterodimer in non-small cell lung cancer. Oncogene 2021;40:2596–609.

69. Regales L, Gong Y, Shen R, de Stanchina E, Vivanco I, Goel A, et al. Dual targeting of EGFR can overcome a major drug resistance mutation in mouse models of EGFR mutant lung cancer. J Clin Invest 2009;119:3000–10.

70. Busser B, Sancey L, Josserand V, Niang C, Khochbin S, Favrot MC, et al. Amphiregulin promotes resistance to gefitinib in nonsmall cell lung cancer cells by regulating Ku70 acetylation. Mol Ther 2010;18:536–43.

71. Busser B, Sancey L, Josserand V, Niang C, Favrot MC, Coll J-L, et al. Amphiregulin promotes BAX inhibition and resistance to gefitinib in non-small-cell lung cancers. Mol Ther 2010;18:528–35.

72. Ishikawa N, Daigo Y, Takano A, Taniwaki M, Kato T, Hayama S, et al. Increases of amphiregulin and transforming growth factor-alpha in serum as predictors of poor response to gefitinib among patients with advanced non-small cell lung cancers. Cancer Res 2005;65:9176–84.

73. Quintanal-Villalonga A, Taniguchi H, Zhan YA, Hasan MM, Chavan SS, Meng F, et al. Comprehensive molecular characterization of lung tumors implicates AKT and MYC signaling in adenocarcinoma to squamous cell transdifferentiation. J Hematol Oncol 2021;14:170.

74. Barton CE, Johnson KN, Mays DM, Boehnke K, Shyr Y, Boukamp P, et al. Novel p63 target genes involved in paracrine signaling and keratinocyte differentiation. Cell Death Dis 2010;1:e74.

75. Wu G, Nomoto S, Hoque MO, Dracheva T, Osada M, Lee C-CR, et al. DeltaN-p63alpha and TAp63alpha regulate transcription of genes with distinct biological functions in cancer and development. Cancer Res 2003;63:2351–7.

76. Bruno R, Proietti A, Alì G, Puppo G, Ribechini A, Chella A, et al. Squamous cell transformation and EGFR T790M mutation as acquired resistance mechanisms in a patient with lung adenocarcinoma treated with a tyrosine kinase inhibitor: a case report. Oncol Lett 2017;14:5947–51.

77. Longo L, Mengoli MC, Bertolini F, Bettelli S, Manfredini S, Rossi G. Synchronous occurrence of squamous-cell carcinoma "transformation" and EGFR exon 20 S768I mutation as a novel mechanism of resistance in EGFR-mutated lung adenocarcinoma. Lung Cancer 2017;103:24–6.

78. Jukna A, Montanari G, Mengoli MC, Cavazza A, Covi M, Barbieri F, et al. Squamous cell carcinoma "transformation" concurrent with secondary T790M mutation in resistant EGFR-mutated adenocarcinomas. J Thorac Oncol 2016;11:e49–51.

79. Haratani K, Hayashi H, Watanabe S, Kaneda H, Yoshida T, Takeda M, et al. Two cases of EGFR mutation-positive lung adenocarcinoma that transformed into squamous cell carcinoma: successful treatment of one case with rociletinib. Ann Oncol 2016;27:200–2.

80. Scher KS, Saldivar J-S, Fishbein M, Marchevsky A, Reckamp KL. EGFR-mutated lung cancer with T790M-acquired resistance in the brain and histologic transformation in the lung. J Natl Compr Canc Netw 2013;11:1040–4.

81. Kuiper JL, Ronden MI, Becker A, Heideman DAM, van Hengel P, Ylstra B, et al. Transformation to a squamous cell carcinoma phenotype of an EGFR-mutated NSCLC patient after treatment with an EGFR-tyrosine kinase inhibitor. J Clin Pathol 2015;68:320–1.

82. Hsieh M-S, Jhuang J-Y, Hua S-F, Chou Y-H. Histologic evolution from adenocarcinoma to squamous cell carcinoma after gefitinib treatment. Ann Thorac Surg 2015;99:316–19.

83. Levin PA, Mayer M, Hoskin S, Sailors J, Oliver DH, Gerber DE. Histologic transformation from adenocarcinoma to squamous cell carcinoma as a mechanism of resistance to EGFR inhibition. J Thorac Oncol 2015;10:e86–8.